Electronic Supplementary Material (ESI) for Green Chemistry.
This journal is © The Royal Society of Chemistry 2018

Electronic supplementary information

Photoelectrochemical driving and clean synthesis of energetic salts of 5, 5'-azotetrazolate at room temperature

Huichao He, [†]* Jinyan Du, [†] Bo Wu, [†] Xiaohui Duan, [†] Yong Zhou, [§]*, Gaili Ke, [†] Tingting Huo, [‡] Qin Ren, [†] Liang Bian, [‡] and Faqin Dong [‡]*

[†]State Key Laboratory of Environmental Friendly Energy Materials, School of Materials Science and Engineering, Southwest University of Science and Technology, Mianyang, Sichuan 621010, P. R. China

[‡]Key Laboratory of Solid Waste Treatment and Resource Recycle of Ministry of Education, Southwest University of Science and Technology, Mianyang, Sichuan 621010, P. R. China

[§]Ecomaterials and Renewable Energy Research Center, School of Physics, National Laboratory of Solid State Microstructures, Nanjing University, Nanjing, Jiangsu 210093, P. R. China

***Corresponding Author** Tel.: +86-0816-2409201; fax: +86-0816-2409201;

E-mail: hehuichao@swust.edu.cn (Huichao He); zhouyong1999@nju.edu.cn (Yong Zhou); fqdong@swust.edu.cn (Faqin Dong).

1 Experimental Section

1.1 Preparation and characterization of W, Mo co-doped $BiVO_4$ film.

The W, Mo co-doped $BiVO_4$ film was prepared by a drop-casting method as reported in our previous work.[1, 2] Briefly, $(NH_4)_6Mo_7O_{24}\cdot 4H_2O$ (Aladdin, 99.9%) and $(NH_4)_{10}W_{12}O_{41}\cdot 5H_2O$ (Aladdin, 99.9%) were dissolved separately at a concentration of 25 mM in ethylene glycol as Mo and W precursor solution. $Bi(NO_3)_3\cdot 5H_2O$ (Aladdin, 99.0%) and NH_4VO_3 (Aladdin, 99.0%) were dissolved separately in concentrated HNO_3 and ethylene glycol (V_{HNO3}: V_{EG}=2:8) to form 50 mM Bi and V precursor solution. Then, the precursor solutions were mixed in a desired atomic ratio of Bi: V: W: Mo=100: 92: 2: 6. 100 μL of mixed precursor solution was drop-cast on a FTO substrate (2.0 cm×2.5 cm, Sheet Resistance<50Ω) that had been cleaned and sonicated with distilled water and ethanol, respectively. After that, the dropped precursor solution was dried in air at 150 ℃ for 45 min and then annealed at 500 °C for 90 min to form W, Mo co-doped $BiVO_4$ film on FTO substrate. To confirm the higher photoelectrochemical activity of W, Mo co-doped $BiVO_4$ film, undoped $BiVO_4$ film was prepared using the same method with precursor solution of an atomic ratio of Bi: V =100: 100.

The as-prepared W, Mo co-doped $BiVO_4$ film was characterized using scanning electron microscopy (SEM, Zeiss Supra 55V), X-ray diffraction spectroscopy (XRD, PANalytical X'pert PRO), X-ray photoelectron spectroscopy (XPS, Kratos AXIS Ultra DLD) and UV-vis spectrometer (Cary 5000). The SEM image shown in **Figure S1** reveals that the as-prepared film has a microstructure of nanoflake arrays with an average thickness of 20 nm and length of 1 μm. The measured XRD patterns confirm that the as-prepared W, Mo co-doped $BiVO_4$ film consists of monoclinic $BiVO_4$

(JCPDS: 01-075-1867) (shown in **Figure S2a**). The surface composition of W, Mo co-doped $BiVO_4$ film was verified by XPS measurement. As shown in **Figure S2b-2e,** the characteristic peaks of Bi $4f_{5/2}$, Bi $4f_{7/2}$, V $2p_{1/2}$, V $2p_{3/2}$, Mo $3d_{3/2}$, Mo $3d_{5/2}$, W 4f $_{5/2}$ and 4f $_{7/2}$ peaks are closely matched the typical peaks of Bi^{3+}, V^{5+}, $Mo^{6+}$and W^{6+} in W, Mo co-doped $BiVO_4$ film. [3] The optical absorption behaviour of W, Mo co-doped $BiVO_4$ film was shown in **Figure S3a**, which indicates the as-prepared film has a band gap of approximately 2.42 eV (**Figure S3b**).

1.2 Synthesis of sodium 5, 5'-azotetrazolate

Sodium 5, 5'-azotetrazolate (SZT) was synthesized by photoelectrochemical approach using W, Mo co-doped $BiVO_4$ film photoanode. A three-electrode cell (quartz cup, 30 mL) was used as reaction vessel. The working electrode was the as-prepared W, Mo co-doped $BiVO_4$ film which was placed with an active area of 4.0 cm^2 for irradiation. The counter electrode was a 0.5 mm diameter Pt wire (99.99%, CHI Instrument) and the reference electrode was saturated Ag/AgCl electrode (*sat.* KCl, CHInstruments). 20 mL of 0.2 M Na_2CO_3-0.1 M 5-amino-1*H*-tetrazole (5AT) water solution was used as electrolyte for the photoelectrochemical synthesis of SZT at room temperature (25℃). The illumination source was a 300 W xenon lamp with AM 1.5G filter (Beijing China Education Au-light *Co.,* Ltd.). The lamp was positioned to provide approximately 150 mW/cm^2 irradiations on the W, Mo co-doped $BiVO_4$ film, the irradiation power was measured by a thermopile detector (Beijing China Education Au-light *Co.,* Ltd.). The photoelectrochemical synthesis of SZT are conducted using back-side illumination (through the FTO substrate to W, Mo co-doped $BiVO_4$ film). A CH Instruments 660E electrochemical workstation was employed to control and record the photoelectrochemical reaction signals. During the photoelectrochemical reaction, the 0.2 M Na_2CO_3-0.1 M 5AT solution was gradually changed from colourless to yellow, indicating SZT formed in the solution. After irradiation of an hour, the temperature of photoelectrochemical cell and electrolyte was increased to ~26.5°C. To avoid the influence of temperature, an intermittent photoelectrochemical reaction route was employed to cool the temperature of photoelectrochemical cell and electrolyte to 25°C after every hour irradiation reaction. After photoelectrochemical reaction, the obtained yellow solution was concentrated at 60°C for 5 h and then placed at a fridge with 5°C to form yellow SZT.5H_2O precipitation. Finally, the SZT.5H_2O precipitation were separated from solution by air pump filtration. The yield of SZT.5H_2O depends on the photoelectrochemical reaction time. After 24 h of photoelectrochemical reaction, 0.208 g SZT.5H_2O was obtained with a yield of 69%. For converting the obtained potential (*vs.* SCE) to RHE (NHE at pH=0), the following equation was used.

$$E_{RHE} = E_{Ag/AgCl} + 0.059\ \mathrm{pH} + E_{Ag/AgCl}{}^{\Theta}\ (E_{Ag/AgCl}{}^{\Theta} = 0.197\ \mathrm{V}\ vs.\ \mathrm{NHE\ at\ 25℃}) \quad (1)$$

To check the possibility that the colour-change of solution was caused by the dissolution or detachment of W, Mo co-doped $BiVO_4$ film during photoelectrochemical reaction, we have performed a comparison experiment in a 5AT-free Na_2CO_3 water solution. The colour of 0.2 M Na_2CO_3 solution is unchanged even after 5 hours photoelectrochemical reaction at 1.23 V vs. RHE (shown in **Figure S6**). Meanwhile, the W, Mo co-doped $BiVO_4$ film is not visibly detached after photoelectrochemical reaction (see the Video), but slight anodic-photocorrosion. The concentration of dissolved Bi and V in the used Na_2CO_3 solution was analysed by inductively coupled plasma technique (ICP, Thermo ICAP6300 Duo). After 5 hours photoelectrochemical reaction at 1.23 V vs. RHE, 1.63 μM V and 1.39 μM Bi were detected in the used Na_2CO_3 electrolyte due to the anodic-photocorrosion of $BiVO_4$ (**see Table S2**). However, the slight anodic-photocorrosion of W, Mo co-doped

$BiVO_4$ film has no influence on the UV-Vis absorption characteristics of Na_2CO_3 solution (**see Figure S6c**).

The formation free energy of 5AT and 5, 5'-azotetrazolate was calculated at 298.15K by density functional theoretical on Materials Studio. The formation free energy of CO_3^{2-} and HCO_3^- was obtained from NIST Chemistry WebBook (http://webbook.nist.gov/). The formation free energy data are shown in **Table S1**. Based on the thermodynamics associated theory, the standard Gibbs free energy of 5AT coupling reaction (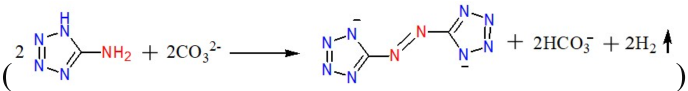) was calculated as follows: $\Delta_r G_m^{\Theta}=\Delta_f G_m^{\Theta}$(5, 5'-azotetrazolate)$+2\Delta_f G_m^{\Theta}(HCO_3^-)+2\Delta_f G_m^{\Theta}(H_2)-2\Delta_f G_m^{\Theta}$(5AT)$-2\Delta_f G_m^{\Theta}(CO_3^{2-})$=-143.4 kJ/mol. The standard potential (E^{Θ}) of 5AT coupling reaction was calculated to be 0.37 V *vs.* RHE through the electrochemical and thermodynamics equation of $\Delta_r G_m^{\Theta}=-z E^{\Theta}F$, where $\Delta_r G_m^{\Theta}$ is the standard Gibbs free energy of reaction, z is the stoichiometric coefficient of reaction (z=4), F is Faraday constant (96484.6 C.mol^{-1}). This result indicates that the 5AT coupling reaction is more favorable than the water oxidation reaction in thermodynamics, because the E^{Θ} of water oxidation reaction (1.23 V *vs.* RHE) is higher than the E^{Θ} of 5AT coupling reaction.

Table S1. The formation free energy data of 5AT, 5, 5'-azotetrazolate, CO_3^{2-}(aq), HCO_3^-(aq) and H_2.

Compound	5AT	5, 5'-azotetrazolate	CO_3^{2-}(aq)	HCO_3^-(aq)	H_2
$\Delta_f G_m^{\Theta}$ (kJ/mol)	19.75	14.02	-527.81	-586.77	0

A spectrophotometric method was employed to analyze the formation amount of SZT during the photoelectrochemical reaction. 2 mL of electrolyte was collected from the photoelectrochemical cell after every hour photoelectrochemical reaction and then analyzed with a UV-Vis spectrophotometer (Shanghai INESA Scientific Instrument *Co.*, *Ltd.*). For comparison, 0.2 M Na_2CO_3-0.1 M 5AT water solution and standard SZT water solution were investigated by UV-Vis spectrophotometry, respectively. The standard SZT was synthesized by traditional method as reported in literatures. [4, 5] The absorption spectrum shows that 0.2 M Na_2CO_3-0.1 M 5AT water solution has no characteristic absorption peak at range of 380-525 nm, whereas the standard SZT solution exhibits an obvious absorption peak at 418 nm (shown in **Figure S4**). Thus, the formation amount of SZT in electrolyte was determined at the characteristic absorption peak of 418 nm. Liquid chromatography (Shimadzu liquid chromatography, LC-20AD) measurements were carried out to detect the purity of SZT solution after photoelectrochemical reaction. The detection was set at 254 nm, and the temperature was controlled at 25°C, using 70% CH_3OH-H_2O as mobile phase.

1.3 Synthesis of guanidinium salts of 5,5'-azotetrazolate

Guanidinium salts of 5,5'-azotetrazolate were synthesized by two steps method. Firstly, sodium 5,5'-azotetrazolate pentahydrate (SZT.5H_2O) as starting material was synthesized by photoelectrochemical method as described in above section. Then, bis(guanidinium) 5, 5'-azotetrazolate (GZT) was synthesized through a simple cation replacement reaction between SZT and guanidine nitrate at 75°C. Similarly, triaminoguanidinium 5, 5'-azotetrazolate (TAGZT) was synthesized through a simple cation replacement reaction between SZT and triaminoguanidinium nitrate at 75°C.

The details of synthesis of GZT and TAGZT are as follows. 0.3775 g of as-prepared SZT.5H_2O was firstly dissolved in deionised water at 75°C, then 0.3050 g guanidine nitrate was added into the SZT.5H_2O solution and dissolved by magnetic stirring. After that, the mixed hot solution was placed at 5°C to induce the formation of GZT. Finally, 0.3253 g GZT were separated from solution by air pump filtration with a yielding of 91%. The synthesizing procedure of TAGZT is similar of GZT, only 0.4175 g triaminoguanidinium nitrate used as cation source compound. 0.4465 g (95% yield) yellow needle-like TAGZT is obtained.

1.4 Characterization of SZT, GZT and TAGZT

The morphology of SZT.5H_2O was characterized by a laser scanning confocal microscope (LeicaTCSSP8). The functional groups of SZT.5H_2O, GZT and TAGZT were determined by FTIR spectrometer (Bruker Tensor 27). The IR measurement range is 4000 cm^{-1} - 400 cm^{-1}, number of scans are 32, spectrum resolution is 4 cm^{-1}. The ^1H and ^{13}C NMR spectra of SZT.5H_2O was recorded with a JEOL Eclipse 400 instrument in D_2O at 25℃. The ^1H and ^{13}C NMR spectra of GZT and TAGZT were recorded with same NMR instrument in DMSO at 25℃. Elemental analyses of GZT and TAGZT were performed with a Vario III EL elementalanalyzer using classical dynamic combustion method.

The photographs of as-prepared GZT and TAGZT products are shown in **Figure S7a** and **S7b**. The GZT are yellow powders and the TAGZT are needle-like yellow compound, which are accordant with the reported works.[5, 6] The FTIR and NMR spectra shown in **Figure S8** reveal that the as-prepared products are GZT and TAGZT, respectively. In the IR spectra, the asymmetric C-N_3 stretching vibration of 5,5'-azotetrazolate anion was observed at 1399 cm^{-1} for the GZT product, and at 1391 cm^{-1} for the TAGZT product, respectively. Simultaneously, the asymmetric C-N_2 stretching mode of azo group appears at 736 cm^{-1} for the GZT product, and at 731 cm^{-1} for the TAGZT product. In addition, the characteristic peaks in the IR spectra are analyzed and shown in **Table S3** and **S4**. In the ^1H NMR spectrum of GZT, a broadened resonance at δ= 7.21 was observed, which caused by NH_2 groups. The signals for NH_2 and NH groups are found at δ= 4.53 ppm and δ=8.65 ppm in the ^1H

NMR spectrum of TAGZT, respectively. Furthermore, the resonance for tetrazole and cation was identified at δ= 173.29 ppm and 158.64 ppm in the ^{13}C NMR spectrum of GZT, respectively. The ^{13}C NMR spectrum of TAGZT shows that the resonance of tetrazole and cation at δ=173.95 ppm and 159.51 ppm, respectively. According to the analyses of IR and NMR spectra, the characteristics of as-prepared products are in well agreement with the structure of GZT and TAGZT (shown inset of **Figure S8a** and **S8b**). The elemental composition for GZT is found to be C: 16.8, N: 78.8, H:4.3, for TAGZT is C:12.7, N:82.2, H: 4.8, which are close with the calculated values of GZT ($C_4H_{12}N_{16}$, 284.25) and TAGZT ($C_4H_{18}N_{22}$, 374.33).

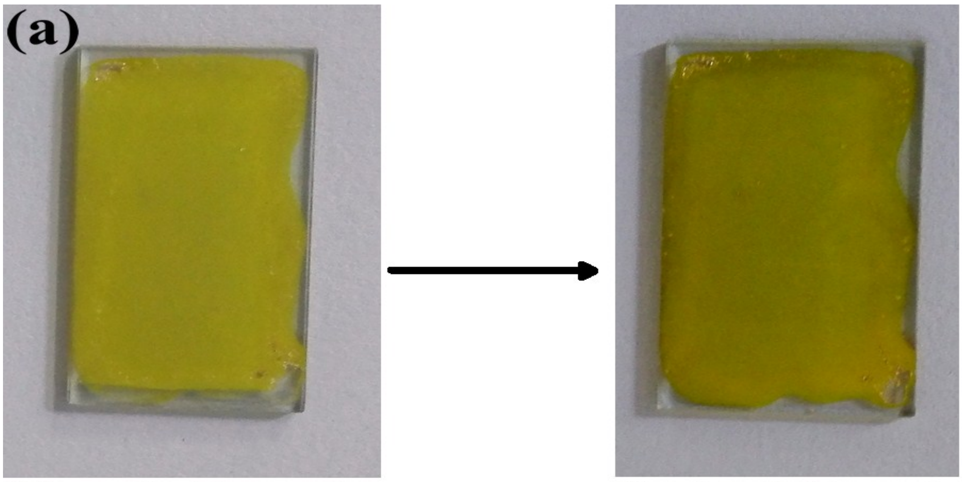

Befor synthesizing reaction

After 8 h synthesizing reaction

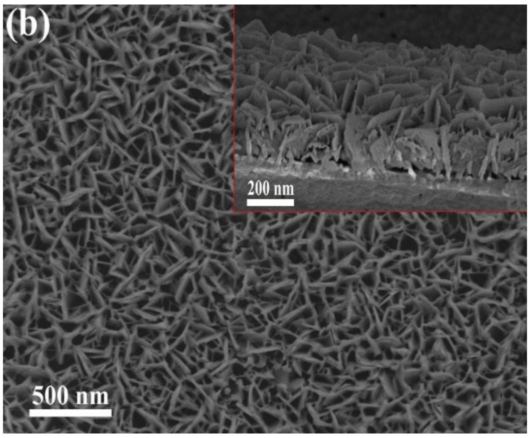

Figure S1. Photograph of a W, Mo co-doped $BiVO_4$ film (a) before and after 8 h photoelectrochemical reaction for SZT synthesizing. (b) SEM image of W, Mo co-doped $BiVO_4$ film.

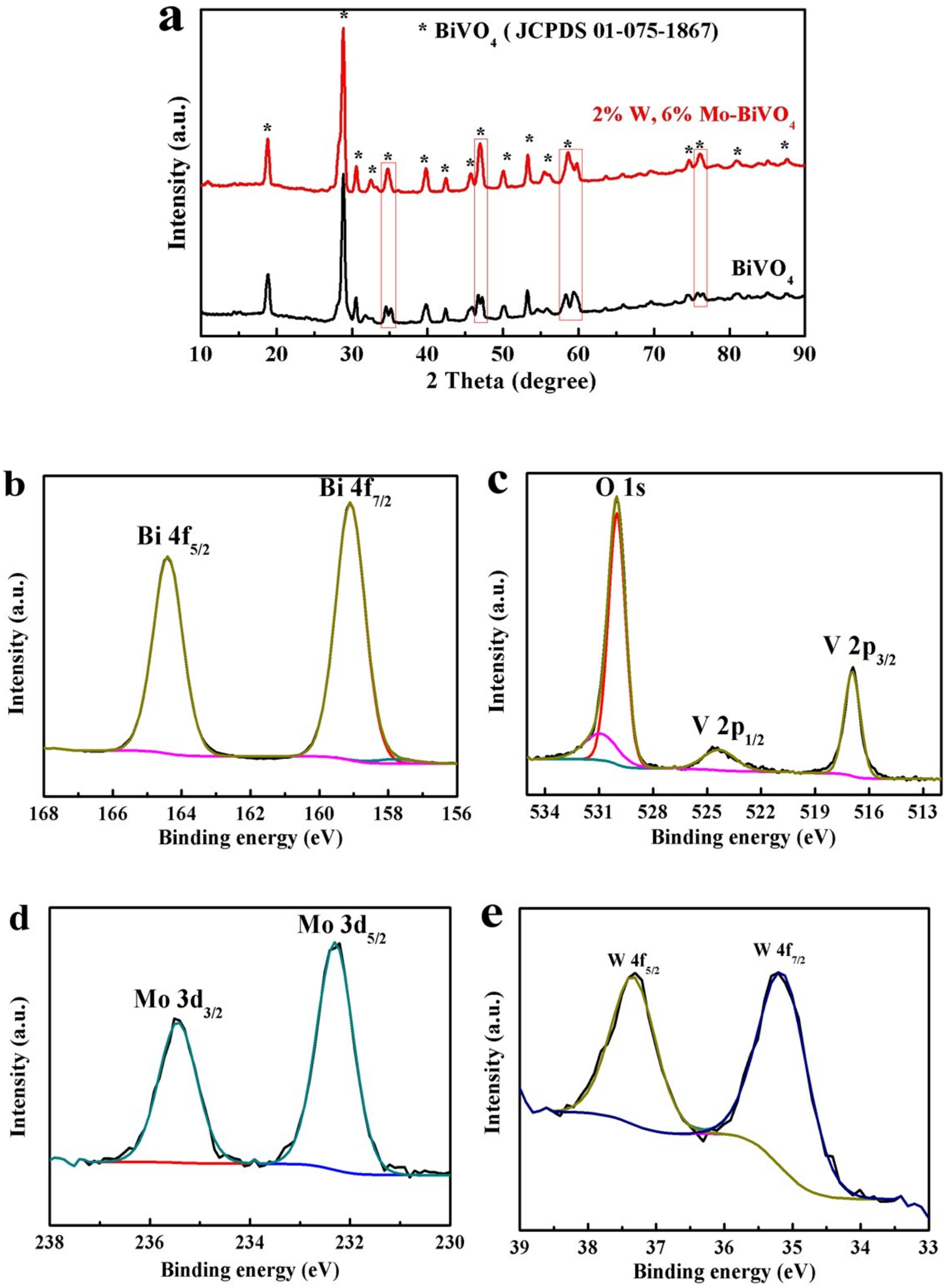

Figure S2. (a) XRD patterns of BiVO$_4$ and W, Mo co-doped BiVO$_4$ film. High resolution XPS spectrum of (b) Bi 4f, (c) O 1s and V 2p, (d) Mo 3d and (e) W 4f for the W, Mo co-doped BiVO$_4$ film.

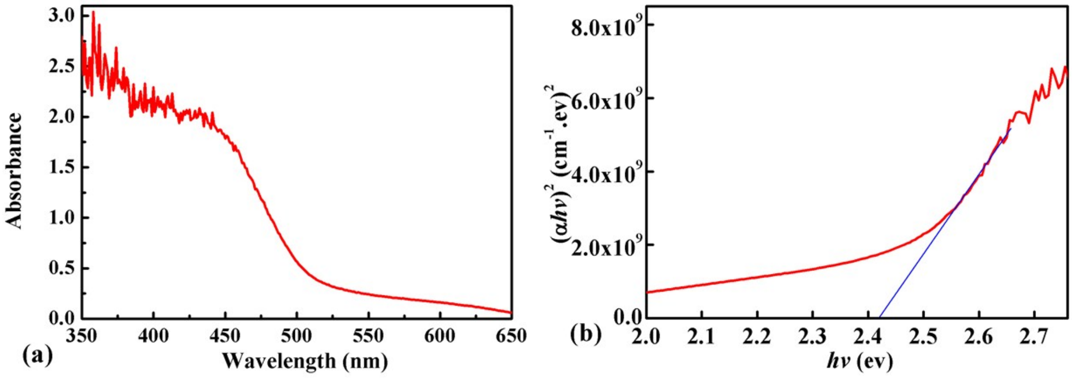

Figure S3 (a) UV-vis absorbance spectrum and (b) Tauc plot of W, Mo co-doped $BiVO_4$ film.

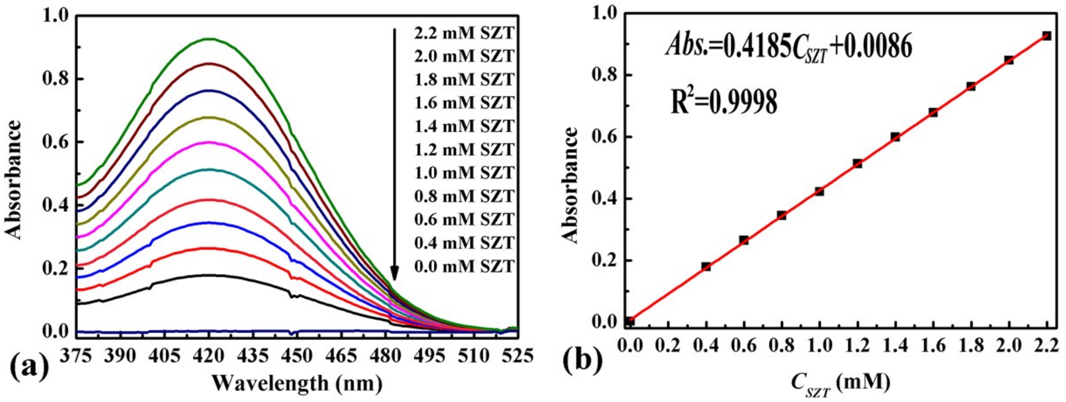

Figure S4 (a) UV-vis absorbance spectra of 0.2 M Na_2CO_3 water solution containing different concentrations of SZT. (b) Linear relationship between absorbance at 419 nm and concentration of SZT.

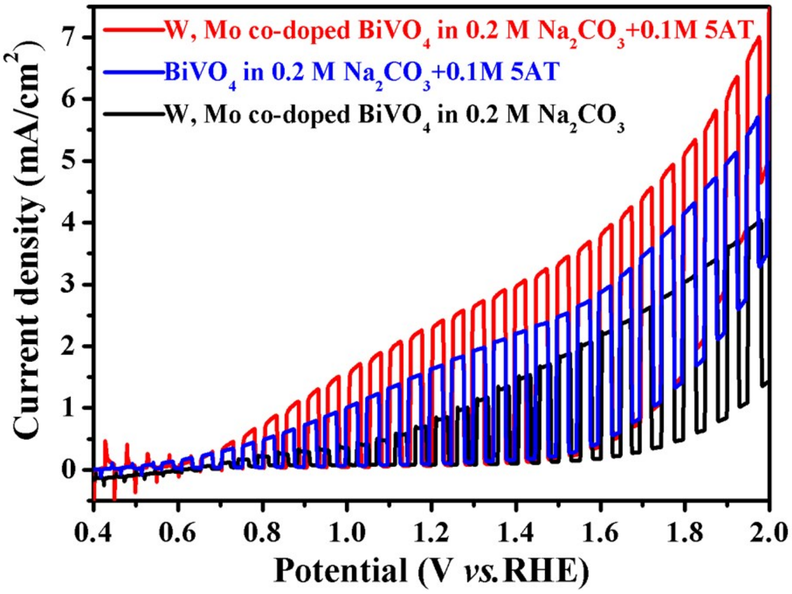

Figure S5. Chopped LSV curves for the W, Mo co-doped and undoped $BiVO_4$ film in 0.2 M Na_2CO_3 (pH 10.3) and 0.2 M Na_2CO_3-0.1 M 5AT water solution (pH 9.3) under intermittent irradiation with 150 mW/cm^2 simulated solar light. The scan rate was 20 mV/s.

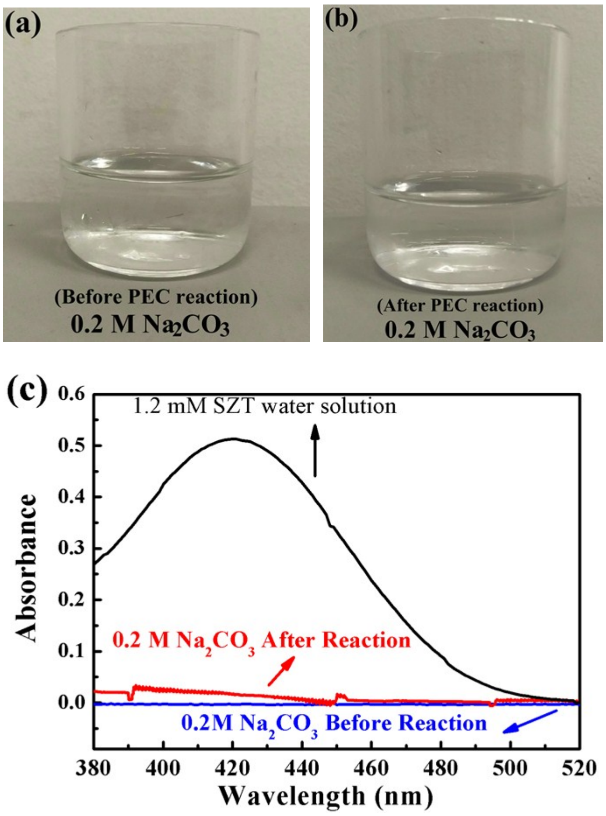

Figure S6 (a) and (b) Photograph of 0.2 M Na_2CO_3 solution before and after 5 hours photoelectrochemical reaction at 1.23 V *vs.* RHE using the W, Mo co-doped $BiVO_4$ photoanode under irradiation with 150 mW/cm^2 simulated solar light. (c) Absorbance spectrum of 0.2 M Na_2CO_3 solution before and after 5 hours photoelectrochemical reaction.

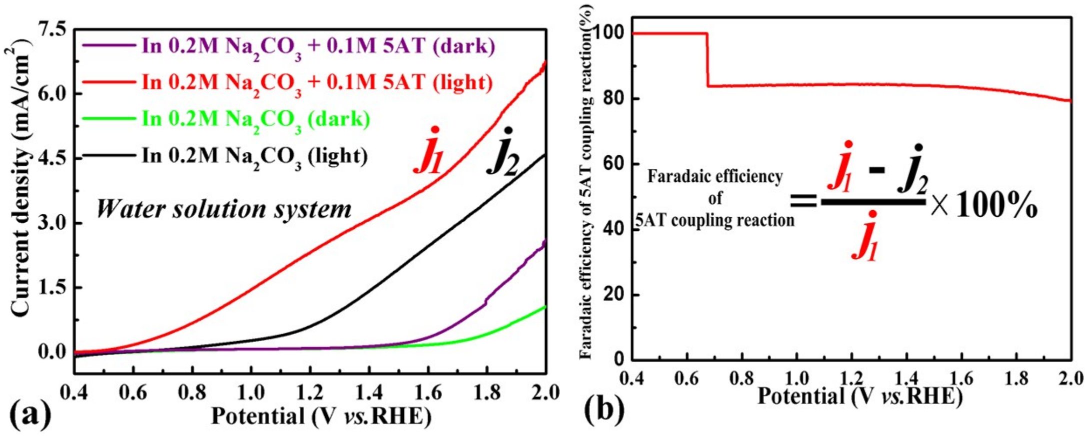

Figure S7 (a) LSV curves for the W, Mo co-doped $BiVO_4$ film in 0.2 M Na_2CO_3 (pH 10.3) and 0.2 M Na_2CO_3-0.1 M 5AT water solution (pH 9.3) without and under irradiation with 150 mW/cm^2 simulated solar light. The scan rate was 20 mV/s. (b) Calculated Faradaic efficiency of 5AT coupling reaction on the basis of data in Figure S5a.

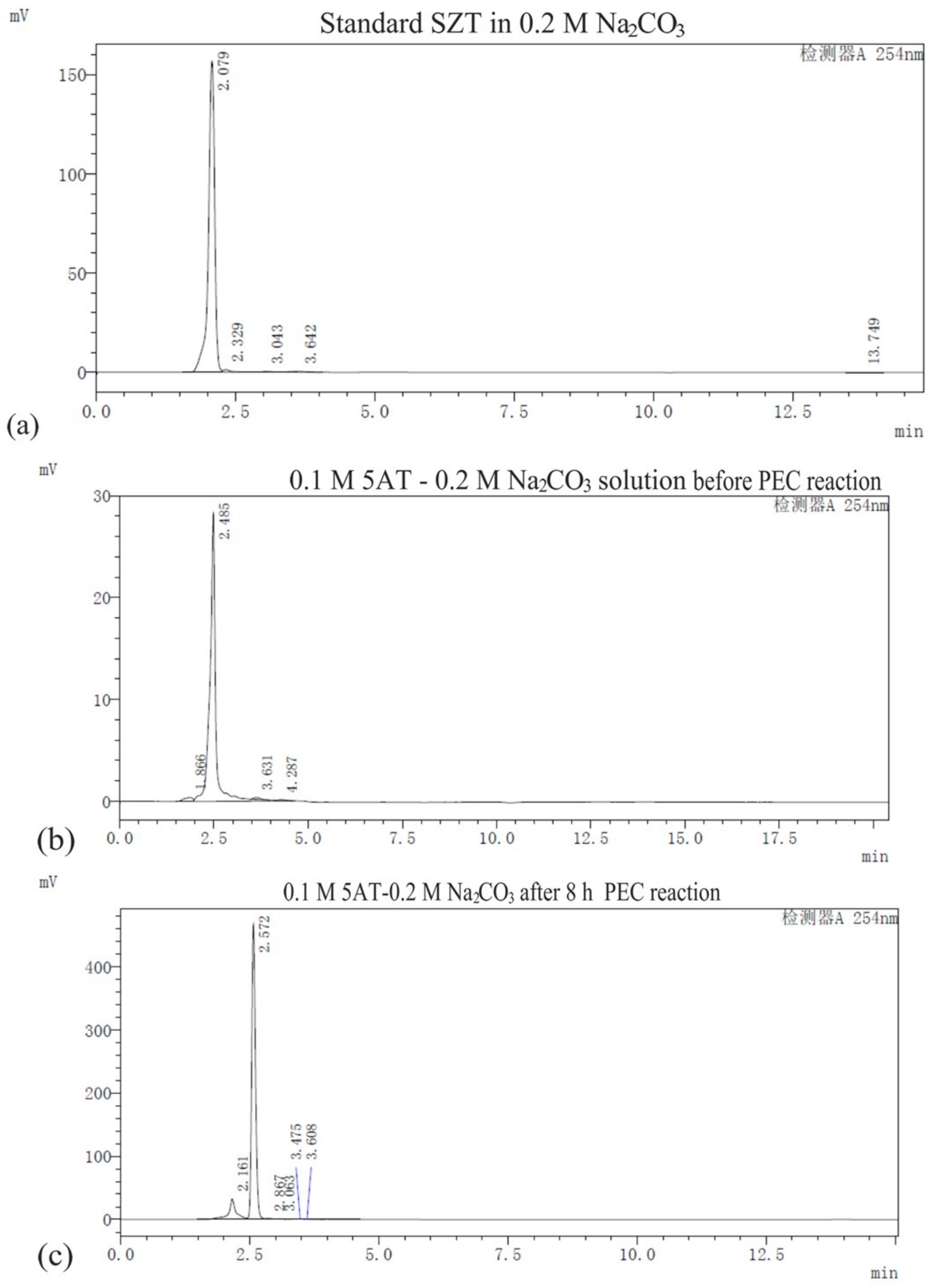

Figure S8 Liquid Chromatography of (a) standard SZT in 0.2M Na_2CO_3, (b) 0.1M 5AT-0.2M Na_2CO_3 before photoelectrochemical reaction, and (c) 0.1M 5AT-0.2M Na_2CO_3 after 8h photoelectrochemical reaction.

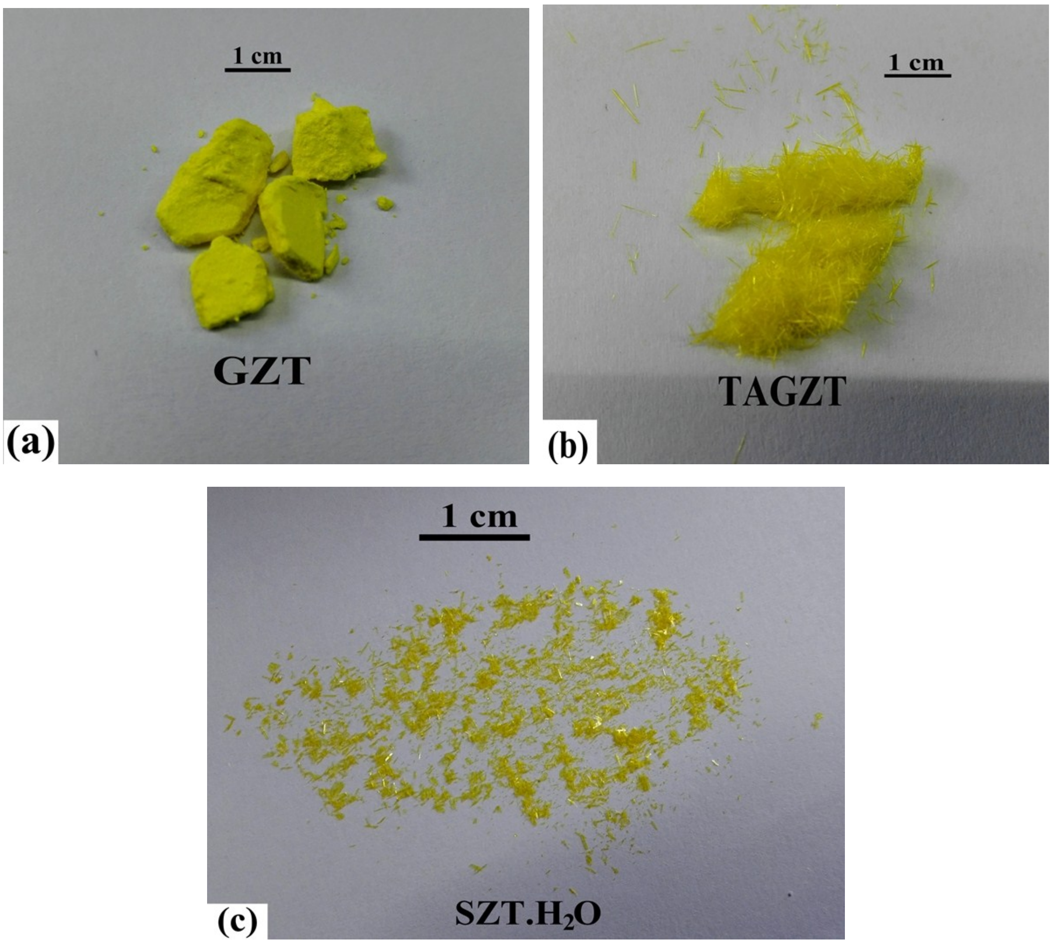

Figure S9 Photograph of the as-prepared (a) GZT, (b) TAGZT and (c) SZT.5H_2O product.

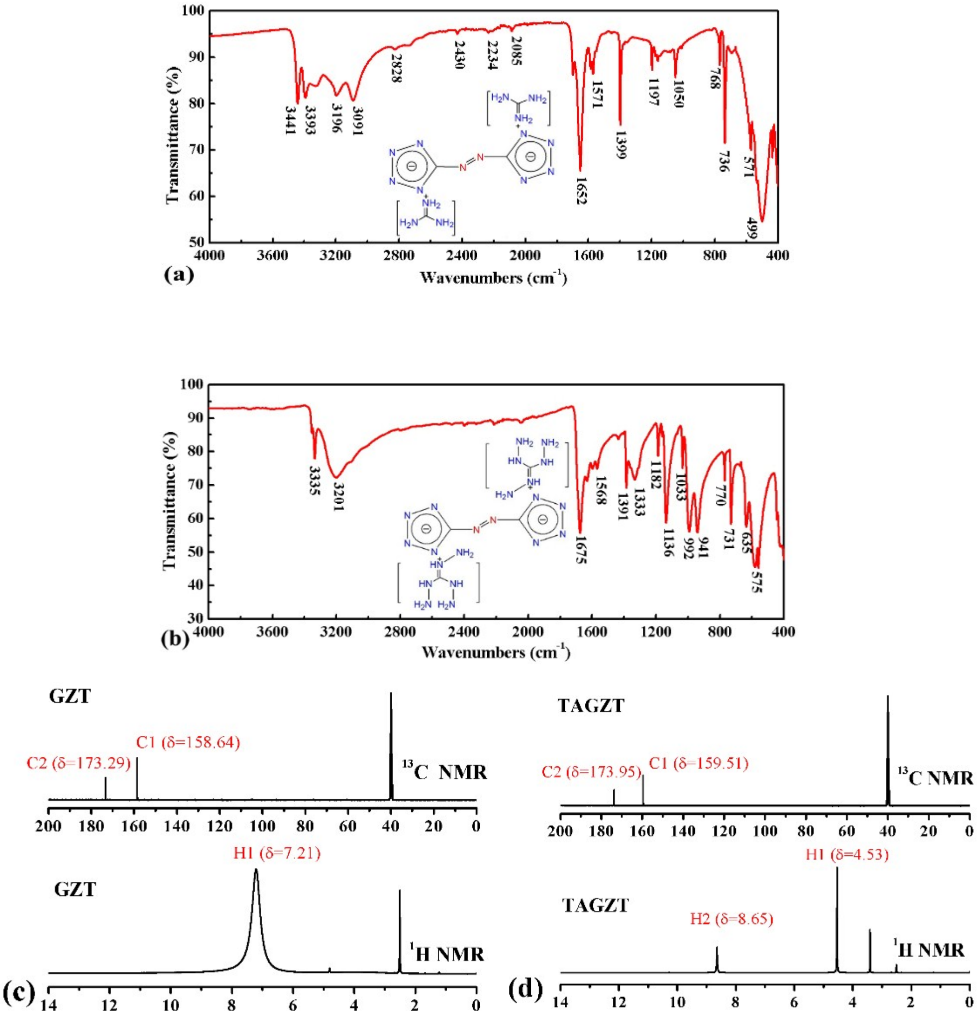

Figure S10 FTIR spectrum of (a) GZT and (b) TAGZT. ^{1}H and ^{13}C NMR spectrum of (c) GZT and (d) TAGZT.

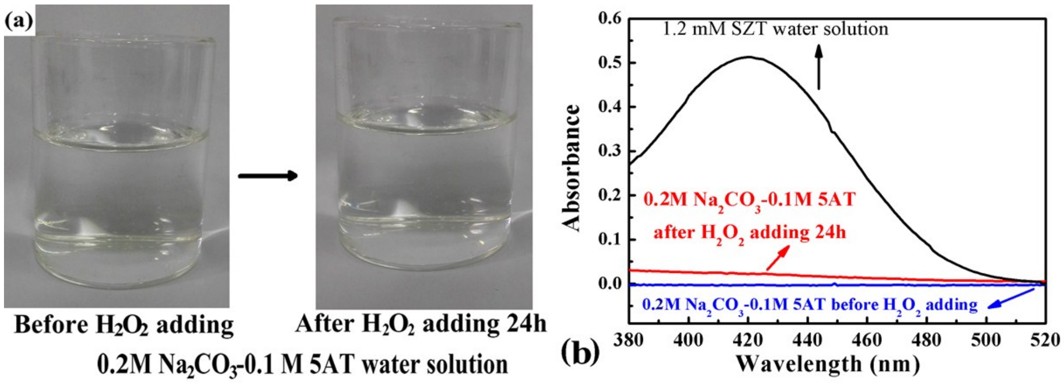

0.2M Na_2CO_3-0.1 M 5AT water solution

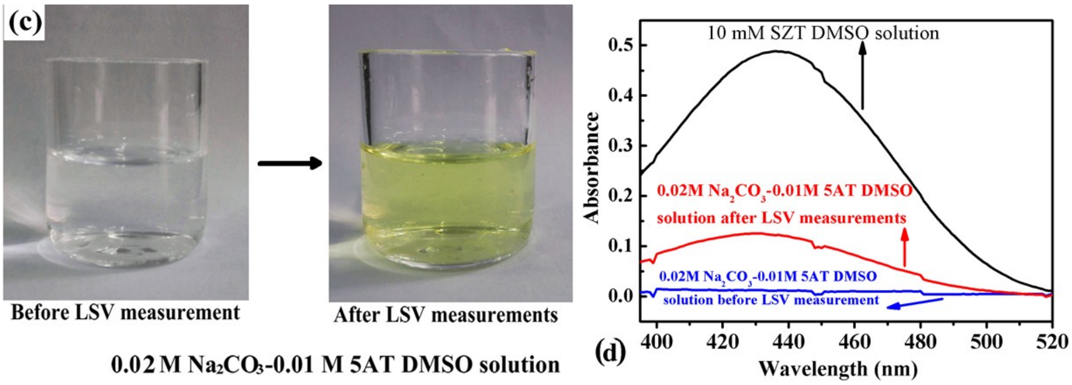

0.02 M Na_2CO_3-0.01 M 5AT DMSO solution

Figure S11 (a) and (c) Photograph of 5AT-based solution before and after the W, Mo co-doped $BiVO_4$ photoanode LSV measurements under irradiation with 150 mW/cm^2 simulated solar light. (b) and (d) Absorbance spectrum of 5AT-based solution before and after LSV measurements.

Table S2 The dissolved concentration of Bi and V in 0.2M Na_2CO_3 solution that used for 5 hours photoelectrochemical reaction at 1.23 V vs. RHE of W, Mo co-doped $BiVO_4$ film.

Element	V	Bi
Concentration(μM)	1.63	1.39

Table S3 The analyzed results of characteristic peaks in the GZT IR spectrum.

Peak of GZT (cm-1)	3441, 3393	3196, 3091	1652	1571	1197, 1050
Bond	υ(NH)	υ(=N$^+$-H)	δ(=N$^+$-H)	δ(NH$_2$)	υ(NCN)

Table S4 The analyzed results of characteristic peaks in the TAGZT IR spectrum.

Peak of TAGZT (cm-1)	3335	3201	1675	1568	1333, 1182, 1033	992, 941
Bond	υ(NH)	υ(=N$^+$-H)	δ(NH)	δ(NH_2)	υ(NCN)	ω(NNH_2), γ(CN)

References

(1) He H. C.; Berglund S. P.; Rettie A.; Chemelewski W.; Xiao P.; Zhang Y. H.; Mullins C. B. *J. Mater. Chem. A,* **2014**, 24, 9371-9379.

(2) He H. C.; Zhou Y.; Ke G. L.; Zhong X. H.; Yang M. J.; Bian L.; Lv K. L.; Dong F. Q. *Electrochim. Acta,* **2017**, 257, 181-191.

(3) Berglund S. P.; Rettie A. J. E.; Hoang S.; Mullins C. B. *Phys. Chem. Chem. Phys.,* **2012**, 14, 7065-7075.

(4) Hiskey M. A.; Goldman N.; Stine J. R. *J. Energetic Mater.,***1998**, 16, 119-127.

(5) Hammerl A.; Holl G.; Klapötke T. M.; Mayer P.; Nöth H.; Piotrowski H.; Warchhold M. *Eur. J. Inorg. Chem.,* **2002**, 4, 834-845.

(6) Hammerl A.; Hiskey M. A.; Holl G.; Klapötke T. M.; Polborn K.; Stierstorfer J.; Weigand J. J. *Chem. Mater.*, 2005, 17, 3784-3793.